Developmental Biology 395 (2014) 120–130

Contents lists available at ScienceDirect

Developmental Biology

journal homepage: www.elsevier.com/locate/developmentalbiology

A one-dimensional model of PCP signaling: Polarized cell behavior in the notochord of the ascidian *Ciona*

Matthew J. Kourakis, Wendy Reeves [1], Erin Newman-Smith, Benoit Maury [2], Sarah Abdul-Wajid, William C. Smith *

Department of Molecular, Cell and Developmental Biology, University of California, Santa Barbara, Santa Barbara, CA 93106, USA

ARTICLE INFO

Article history:
Received 2 May 2014
Received in revised form
25 July 2014
Accepted 19 August 2014
Available online 28 August 2014

Keywords:
PCP
Notochord development
Cell polarity
Ciona

ABSTRACT

Despite its importance in development and physiology the planar cell polarity (PCP) pathway remains one of the most enigmatic signaling mechanisms. The notochord of the ascidian *Ciona* provides a unique model for investigating the PCP pathway. Interestingly, the notochord appears to be the only embryonic structure in *Ciona* activating the PCP pathway. Moreover, the *Ciona* notochord as a single-file array of forty polarized cells is a uniquely tractable system for the study of polarization dynamics and the transmission of the PCP pathway. Here, we test models for propagation of a polarizing signal, interrogating temporal, spatial and signaling requirements. A simple cell–cell relay cascading through the entire length of the notochord is not supported; instead a more complex mechanism is revealed, with interactions influencing polarity between neighboring cells, but not distant ones. Mechanisms coordinating notochord-wide polarity remain elusive, but appear to entrain general (i.e., global) polarity even while local interactions remain important. However, this global polarizer does not appear to act as a localized, spatially-restricted determinant. Coordination of polarity along the long axis of the notochord requires the PCP pathway, a role we demonstrate is temporally distinct from this pathway's earlier role in convergent extension and intercalation. We also reveal polarity in the notochord to be dynamic: a cell's polarity state can be changed and then restored, underscoring the *Ciona* notochord's amenability for in vivo studies of PCP.

Introduction

Oriented cell morphology is an essential feature of animal development and physiology, but mechanisms governing the transmission of polarity at the tissue level remain unresolved (Bertet and Lecuit, 2009). The polarity defined by the apical–basal axis of an epithelium, for example, is important for the proper function of that tissue, partitioning tasks of the surface from those on the inside or luminal space. Perpendicular to the apical–basal orientation, along the surface of the epithelium, cells also show coordinated polarity in the planar axis. The polarity of a sheet of cells, or planar cell polarity (PCP), can be seen in examples such as the regular orientation of trichomes and bristles in the cuticle of *Drosophila*, the pattern of ommatidia in the compound eye or, in mammals, the arrangement of sensory hair cells in the inner ear and the pattern of hair follicles and associated structures within the epidermis (Chang and Nathans, 2013; Ezan and Montcouquiol, 2013; Goodrich and Strutt, 2011; Seifert and Mlodzik, 2007; Wang and Nathans, 2007). In these diverse examples a common genetic pathway, the PCP pathway, is used to orient cells in an epithelium. Key shared components of this pathway include the transmembrane proteins Frizzled (Fz) and Strabismus (Stbm; also called Van Gogh) and the cytoplasmic proteins Prickle (Pk) and Dishevelled (Dsh). In cells of the fly wing disc a regular pattern of these proteins (and others) is established when a subset of these proteins, asymmetrically localized to the proximal membrane and cortex, interacts and reinforces interactions with still another subset localized to the distal side of the adjoining cell, and so on, in iterated fashion.

Many questions remain concerning the mechanisms governing PCP. Investigations of PCP in *Drosophila*, for example, reveal possible sequential or parallel interactions between the so-called "core" set of PCP genes, including proteins like Fz, Stbm, Pk and Dsh, with genes of the "global" module, including Fat, Dachsous and Four-jointed (Axelrod and Tomlin, 2011; Casal et al., 2006).

* Corresponding author.
E-mail address: william.smith@lifesci.ucsb.edu (W.C. Smith).
[1] Present address: Molecular and Cellular Biology, Kansas State University, 116 Ackert Hall, Manhattan, KS 66506, USA.
[2] Present address: UFR des sciences de la santé, Université de Versailles Saint Quentin, 78180 Montigny-le-Bretonneux, France.

http://dx.doi.org/10.1016/j.ydbio.2014.08.023
0012-1606/

While analyses of mutants demonstrate how these modules affect polarity, whether autonomously or non-autonomously, and reveal epistatic relationships between players, the coordination and propagation of polarity on a *tissue-wide* scale is less well understood. Here we use an invertebrate chordate, the ascidian *Ciona*, to study oriented cell behavior and the propagation of polarizing signal in the context of a key feature of its anatomy, the notochord. The notochord is the defining character of the chordate phylum and, though it acts as an organizing center in vertebrates, its primitive function was likely to provide stiffness along the rostral–caudal axis of the swimming larva (Stemple, 2005). The ascidian notochord is a comparatively new model for planar polarity (Jiang et al., 2005; Shi et al., 2009) and is not, in fact, an epithelial sheet but a single-file rod of exactly forty cells. In this communication, we show that it has unique properties for the study of polarized cell behavior, including amenability to in vivo assays of polarization dynamics, and a simple geometry to investigate the mechanisms governing the transmission of polarizing signals.

The polarity of the *Ciona* notochord was first noted in the orderly placement of nuclei to posterior cell membranes along its length (Jiang et al., 2005). The nuclei of all notochord cells are tightly apposed to its posterior membrane, with the exception of the final, caudal-most nucleus, which is usually positioned at the anterior membrane (Jiang and Smith, 2007). Nuclear position provides a convenient in vivo morphological read-out of polarity in the notochord, making possible a live record of polarization dynamics. This polarity of the nuclei has been found to depend – like the bristles of *Drosophila* and the sensory hair cells of the mammalian ear – on asymmetrically localized molecular components of the PCP pathway, such as Pk and Stbm (Jiang et al., 2005).

The *Ciona* PCP pathway is likely to closely resemble the vertebrate PCP pathway given a comparatively recent shared ancestry, but offers a much simpler system morphologically and genetically. In addition to its known asymmetric localization, the Pk protein has a demonstrated PCP function in ascidian; a spontaneous deletion in the *pk* gene of *Ciona savignyi* leads to defects in both mediolateral (M/L) intercalation and in anterior–posterior (A/P) notochord polarity (Jiang et al., 2005). In this mutant, called *aimless* (*aim*), many notochord cells fail to complete intercalation and cells that intercalate properly have a high incidence of mispolarized nuclei (positioned at the cell anterior membrane instead of the posterior). How this perturbed nuclear polarity is established has not been determined, but the asymmetric protein localization of PCP components is also disrupted in $aim^{-/-}$ notochord cells (Jiang et al., 2005). Conversely, Jiang et al. demonstrated that PCP localization in *aim* can be rescued through electroporation of a *pk*-containing construct. The *aim* mutant, therefore, underscores a tight correlation between PCP function and localization and nuclear localization, showing that these two elements, molecular and morphological, are aspects of the same inherent polarity seen in notochord cells.

Here, we investigate the behavior of *Ciona* notochord cells: the establishment of polarity within notochord cells following intercalation, the directional cell-to-cell transmission properties of this polarity, and the ability of cells to recover proper polarity following experimental perturbation. We present a model in which notochord cell polarity is influenced locally, through the interactions of neighboring cells, but is ultimately coordinated and kept in register through the action of a global polarizer.

Material and methods

Animal culture

Adult *Ciona intestinalis* or *C. savignyi* were collected from Santa Barbara yacht harbor or purchased from M-REP (Carlsbad, CA, USA) and kept at a facility supplied with raw seawater at the University of California, Santa Barbara. Stable transgenic lines carrying the *Brachyury* (*Bra*) promoter (Corbo et al., 1997) driving expression of green fluorescent protein (GFP) in the notochord were generated for both *C. savignyi* and *C. intestinalis* as previously described (Deschet et al., 2003; Joly et al., 2007).

Gametes were isolated, fertilized and dechorionated as described previously (Hendrickson et al., 2004; Veeman et al., 2011). Developmental stages follow the anatomical landmarks given by Hotta et al. (2007); when hours post fertilization (hpf) are given, the temperature of development is 18 °C.

Plasmid constructs

The *C. intestinalis Tensin* promoter (−1392 to +13 of gene KH2012:KH.C9.28) was PCR-amplified using the oligonucleotides CTCGAGAGCATGCGCACTAATCG and AAGCTTCGTCTTCTCTCATTGCTCTG, and then cloned into pSP72BSSPE -SwaI-RFA-Venus (Roure et al., 2007). Next, the first 1113 bp of *C. intestinalis Dsh* (KH2012:KH.L141.37) cDNA (excluding the DEP and C terminus) was PCR amplified using the oligonucleotides ATGTCGGATGAAACGAAAATAGTTTATTATC and AGCTCCCATATCAGTGCATG and cloned into pDONR221. These constructs were then combined with LR clonase (Invitrogen) to produce *Tensin > dnDSH::Venus*.

Tensin > H2A::RFP and *Bra > H2A::RFP* was made using a Gateway (Invitrogen) entry clone containing Histone 2A (H2A) RFP recombined with *Tensin* (*Tens*) promoter-RfA and *Brachyury* promoter-RfA plasmids (Roure et al., 2007).

The expression construct containing the *Brachyury* upstream regulatory region to drive expression of myc-tagged Pk (*Bra > Pk::myc*) was generated previously (Jiang et al., 2005).

Transgenics and electroporations

Transient transgenic animals were generated as described previously (Christiaen et al., 2009) using a BioRad Gene Pulser. Plasmid was introduced at amounts as little as 7.5 μg (*Bra > Pk::myc*) to as high as 70 μg (*Tens > dnDSH::Venus*).

Cells and nuclei are labeled either by using a stable transgenic line carrying GFP driven by the *Brachyury cis*-regulatory element [*Bra > GFP*; (Corbo et al., 1997; Joly et al., 2007)] or by transient expression of this construct by electroporation, which frequently results in mosaic expression. While this GFP does not carry a nuclear localization signal it accumulates around the nucleus. We have confirmed this observation with a Histone 2A-tagged red fluorescent protein construct (our unpublished result).

Prickle morpholino oligonucleotide and microinjections

The full length mRNA of *C. intestinalis prickle* (AB 036840) was used to design a 25-mer morpholino oligonucleotide (Gene Tools, Ltd.) complementary to the ATG translation start site (GCCGCTGGCATGGTCATAAGACTGT). Initial injections were performed on single-cell zygotes to confirm that the MO could phenocopy the pk-null mutant (*aimless*). A control morpholino was injected at equal concentration (CCTCTTACCTCAGTTACAATTTATA) to assay for non-specific effects including, toxicity of the co-injected fast green tracer. Injections at 2- and 4-cell stages included 1–10 mg/ml 10 KDa-Alexa Fluor 568 dextran amine (Invitrogen) so that the presence of the morpholino in any given cell could be confirmed. Morpholino injections were performed as described previously (Yamada et al., 2003).

Immunohistochemistry

To enhance visualization of the *Tensin > dnDSH::Venus* construct, electroporated embryos at the desired developmental stage were fixed in 2% paraformaldehyde in sea water for 1 h then washed four times in PBST, 10 min each. Embryos were incubated in PBST+5% goat serum for 1 h at room temperature or overnight at 4 °C with rabbit anti-red fluorescent- or mouse anti-green-fluorescent protein antibodies (Invitrogen), diluted 1:1000. Animals were washed 5 × for 10 min PBST and then incubated with anti-rabbit Alexa Fluor 546 and anti-mouse Alexa Fluor 688 (Invitrogen), 1:1000, in PBST+5% goat serum for 1 h at room temperature or overnight at 4 °C. Samples were washed 10 × in PBST following secondary incubation. After 1 wash in PBST, samples were incubated in BODIPY FL phallacidin (Invitrogen), 1:100, in PBST for 30 min and washed 4 × in PBST.

Image analysis and microscopy

Live embryos were either viewed directly in a glass-bottom Petri dish or on a slide under a cover slip using a reinforcement label (Avery, 5729) as a spacer. Fixed embryos were immobilized onto a cover slip coated with 0.08% poly-L-lysine, then cleared in 80% glycerol or 1:2 benzyl alcohol:benzyl benzoate (BABB).

Fluorescent and DIC images, including time lapse movies, were taken using a Leica DMRB upright using Slidebook v. 4 or an Olympus IX81 inverted using Slidebook v. 5. Confocal images were captured on an Olympus Fluoview 1000 laser scanning microscope and images analyzed using Imaris software, v. x64, z6.4.0.

To quantify labeling intensity for *Bra > pk::myc* electroporated animals, we used the Plot Profile function in the image processing package Fiji (Schindelin et al., 2012).

Laser ablation and tail bisection

Laser ablations of notochord cells were performed on an Olympus Fluoview 1000 MPE using two-photon femtosecond pulsed laser MaiTai HP (Newport Spectra Physics). The cells to be ablated were scanned with high laser power (1–2 W/950 nm) at a 200 μs/pixel scan speed. The localized scanning resulted in visible rupturing of the cells.

Tail bisections were performed in petri dishes coated with 1% seawater-agarose (Fisher) using a small length (~1 cM) of 0.001 tungsten wire (California Fine Wire Company) secured with beeswax to the end of a Pasteur pipette, sharpened under a flame from a Bunsen burner.

Results

Ciona notochord cells show mediolateral polarity followed by anterior–posterior polarity

In ascidians, notochord progenitors are specified by the sixty-four cell stage (Nakatani and Nishida, 1999). At neurula stage the 40 notochord precursor cells lie in a disk-shaped plate underlying the embryonic neural tube (Fig. 1). As embryogenesis proceeds, cells in the plate intercalate, and in a process similar to that governing the medial migration of mesoderm during vertebrate convergent extension (Keller et al., 2000; Wallingford et al., 2002), mediolaterally-biased lamellipodia direct cells to form a single-file stack of 40 flat, disk-shaped cells (Jiang and Smith, 2007; Munro and Odell, 2002) (stage 21, Fig. 1). During the 4–5 h following the completion of intercalation, notochord cells elongate in the A/P axis, adopting a barrel shape, in concert with the lengthening of the entire embryo (stage 23, Fig. 1; (Hotta et al., 2007)).

In the transition between the completion of intercalation and the initiation of elongation, notochord nuclei are tightly sandwiched between anterior and posterior cell membranes (Figs. 1 and 2). As elongation of the notochord progresses, however, an anterior/posterior (A/P) polarization of the cells becomes apparent through the position of nuclei (Fig. 2A). All nuclei [shown here in a stable transgenic line carrying GFP driven by the *Brachyury cis*-regulatory element (*Bra > GFP*; Corbo et al., 1997)] are found at the posterior pole of each notochord cell, with the exception of the posterior-most nucleus, which is usually found against the anterior membrane (lower inset, Fig. 2A). Time-lapse imaging shows the progression of nuclei polarization as notochord cells elongate (Fig. 2B–D). The nuclei, seen here in notochord cells labeled mosaically by electroporation of *Bra > GFP* (Christiaen et al., 2009), extend across the A/P length of the elongating cells – as if stretched – and then retract to the posterior pole by late stage 23 (Hotta et al., 2007) (Fig. 2D and Suppl. Movie 1). This stretching/receding behavior by notochord nuclei occurs more or less simultaneously along the length of the tail.

Supplementary material related to this article can be found online at http://dx.doi.org/10.1016/j.ydbio.2014.08.023.

The fidelity of this process is high: 98.7% of the non-tip cells ($n=1867$) at stage 23 were observed to contain posteriorly positioned nuclei (Fig. 3). The exception to this rule is the notochord cell at the posterior tip: its nucleus was usually observed in the opposite orientation, at the anterior cell membrane. We observed this relative inversion in 76.2% of posterior tip cells examined ($n=63$) (Fig. 3). This does not appear to be a general property of tip cells, as nuclei were posteriorly localized in 92.2% ($n=51$) of anterior tip cells.

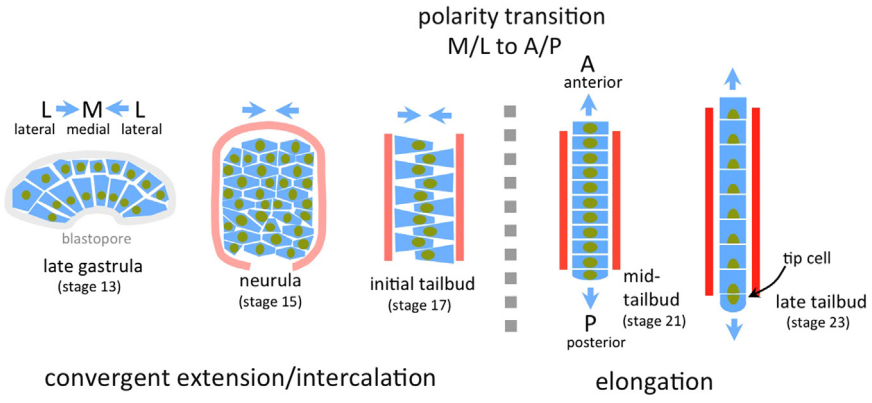

Fig. 1. Model of *Ciona* notochord morphogenesis. Two distinct phases are seen: convergent extension, in which the cells are mediolaterally (M/L) polarized, and elongation, during which the cells show anterior/posterior (A/P) polarization. Stages are according to (Hotta et al., 2007).

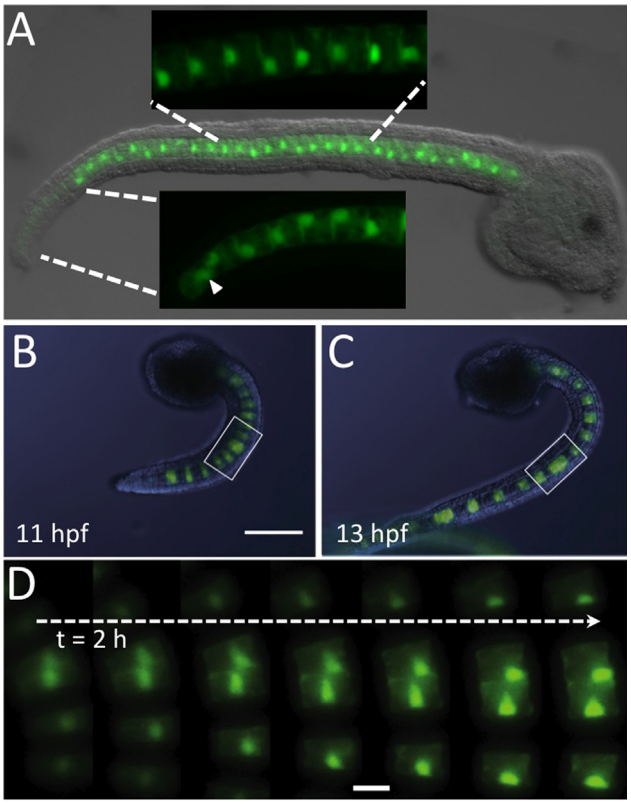

Fig. 2. (A) Polarization of the *Ciona* notochord in the anterior/posterior axis. Nuclei are labeled green with GFP expressed from a stable transgenic construct. Note the nucleus of the posterior-most cell is reversed relative to the other cells (arrowhead, lower inset). (B) and (C) Elongation of the tail and notochord of *Ciona* tailbud embryos over the course of 2 h. The notochord is labeled mosaically (approximately every other cell) with an electroporated GFP construct. (D) Time lapse images taken over a 2 h period at 20 min intervals, showing the polarization of notochord cell nuclei; nuclei first are shown to span the A/P axis of the elongating cell, then they rapidly recede from the anterior, taking their position at the posterior membrane of the cell.

Prickle becomes localized shortly after intercalation

The A/P polarization of notochord cells is evident in both the position of nuclei and the localization of the PCP protein Pk (Jiang et al., 2005). To visualize Pk localization in the notochord during the events of cell elongation and nuclear polarization, we used a previously described expression construct (*Bra > Pk::myc*) to drive mosaic expression of myc-tagged Pk (Jiang et al., 2005). During mediolateral intercalation (stage 19), *Bra > Pk::myc* was seen primarily around the periphery of the cells, with no apparent M/L or A/P localization (Fig. 4A). We had previously reported that Pk::myc was excluded from the basal/lateral edges of intercalating cells (Jiang et al., 2005). However the present result, collected by confocal microscopy rather than epifluorescence, contradicts this earlier result, and we conclude now that no asymmetric mediolateral localization of Pk::myc is evident during intercalation.

At the immediate completion of intercalation (stage 21, Fig. 4B) Pk::myc was strongest at the basal/lateral edges of the cells, with no apparent A/P polarization (Fig. 4B). However, less than an hour later, at stage 22, Pk::myc was localized to the anterior edge of each notochord cell (arrowheads, Fig. 4C), with continued expression at the basal/lateral edges. As elongation progressed, Pk::myc localization became restricted to a concentric domain at the anterior face of the cell [arrowhead, Fig. 4D; (Jiang et al., 2005)]. Quantification of Pk::myc fluorescence along the anterior/posterior axis of notochord cells confirmed a distinct transition in localization between stages 21 and 22 (Fig. 4B′ and C′).

Coordinated polarity is disrupted in aimless, even as local polarity persists

The *aimless (aim)* mutant line in the species *C. savignyi* has a deletion in the *pk* gene predicted to cause a null phenotype (Jiang et al., 2005). In homozygous *aim* embryos (*aim/aim*) notochord cells do not intercalate properly. The notochords of most *aim* embryos, however, have a segment of cells, usually at the posterior, that successfully complete intercalation, forming a single-file column which ranges from a few, to ten or more cells in length (Fig. 5A). In a screen of 68 fully intercalated cells in 8 *aim/aim* embryos, 46% of nuclei were found to be anterior, while 41% were posterior (and 13% were either cytoplasmic with no apparent contact with cell membranes, or stretched between the two poles), indicating that the localization of the nuclei to the anterior or posterior poles is random in *aim* embryos (Fig. 3). These results indicate that despite the loss of Pk, each notochord cell nucleus displays a polarity (i.e., its nucleus not found in the middle of the cell) indicating that the PCP pathway is not required for polarity itself, but rather for coordinated directionality of polarity between cells. We have also observed disruption to the cytoskeleton of fully intercalated notochord cells in *aim/aim* embryos (manuscript in preparation).

While the final placement of nuclei in *aimless* appears random, the development of nuclear polarity within the elongating notochord occurs similarly whether a nucleus comes to be positioned posteriorly – as in wild type – or anteriorly. In either case, the same initial stretching of the nucleus across the A/P axis of the cell is following by retraction of the nucleus toward the membrane where it will come to reside (Fig. 5B).

Cells in the *aim* mutant lack Pk activity throughout embryogenesis, raising the possibility that the A/P polarity defects seen in the tailbud embryo could be the result of an earlier disruption of the PCP pathway, and not necessarily the loss of PCP activity at the elongation stage when A/P polarity becomes evident. To investigate this possibility and the requirement of the core PCP component Dsh in A/P polarity, we made a dominant negative version of *C. intestinalis Dsh* (dnDSH) based on a construct from *Drosophila* (Axelrod et al., 1998). The *dnDSH* cDNA was placed next to the *cis*-regulatory region of the *Ciona Tensin* gene (*Tensin > dnDSH::Venus*), and then expressed mosaically in the notochord by electroporation. The *Tensin cis*-regulatory region (Hotta et al., 1999) does not initiate transcription until mid-tailbud stage, in contrast to the *Brachyury* promoter, which initiates pre-intercalation (Fig. 5C), allowing us to assess the effects of the dnDSH in post-intercalation notochord cells. Expression from the *Tensin* construct rarely caused defects in intercalation, consistent with the developmental timing of the promoter, but after intercalation 12% of cells expressing *dnDSH* were observed to have mislocalized (i.e., anterior) nuclei (Figs. 3 and 5D; $n = 182$ *dnDSH*—expressing cells scored). Control embryos expressing Venus under the *Tensin* promoter showed only 1 of 75 cells scored (1.3%) to have an anteriorly-localized nucleus. Based on our results with *aim* mutants, where a *complete* loss of Pk results in a randomization of polarity and thus half of nuclei continuing to show posterior localization (as in wild type) along with half showing aberrant anterior localization, it is likely that although 12% of cells show visible mislocation of nuclei when positive for *Tensin > dnDSH::Venus*, other positive cells may have disrupted polarity, but posterior nuclei. Nonetheless, cells expressing the dnDSH show a less penetrant phenotype than do cells in *aim* embryos, perhaps due to the relatively late onset of the construct, which likely results in relatively low levels of the dominant negative protein relative to the endogenous DSH.

Core PCP regulates short-range coordination of cells

To test models of cell-to-cell signaling in the establishment of notochord A/P polarity we used a morpholino oligonucleotide

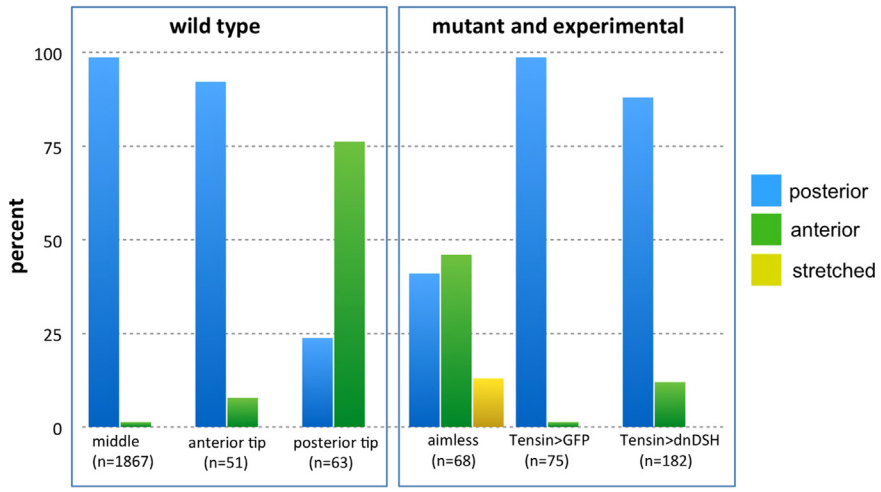

Fig. 3. Quantification of nuclei position in the middle, and the anterior and posterior tip cells of wildtype stage 23 embryos (left panel). The position of nuclei in stage 23 embryos homozygous for a null mutation in *pk* (*aimless*), and embryos electroporated with a construct with the *Tensin* promoter driving a dominant negative version of disheveled (dnDSH) or Venus (negative control) is shown in the right panel.

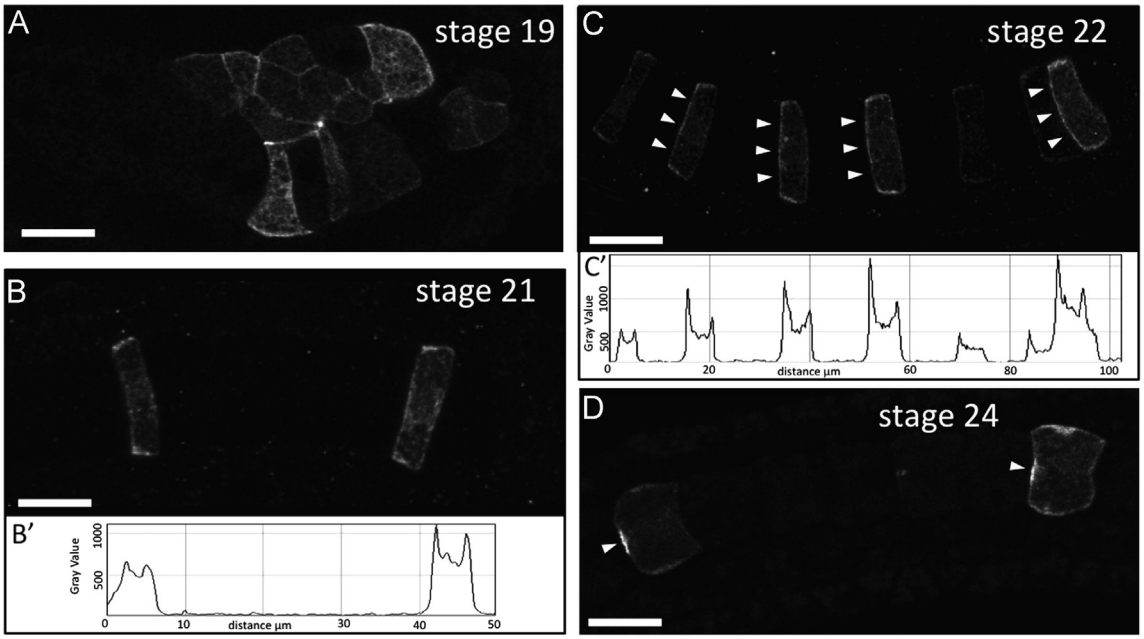

Fig. 4. (A–D) Notochord cells mosaically expressing an electroporated construct containing the *Brachyury* promoter driving Prickle-myc (*Bra > Pk::myc*). The time course of sub-cellular localization of *Pk::myc* from mid-intercalation (stage 19) through elongation (stage 23) is shown. Anterior is to the left for all panels. Arrowheads in C indicates localized *Pk::myc*, and arrowhead in D indicates concentrated localization at the center of the anterior face of the cell. Scale bars are 10 µm. Graphs of fluorescence intensity (generated using Fiji) across the anterior/posterior axis for the cells shown at stages 21 and 22 (C′ and D′).

(MO) targeting the translation start site of *pk*. When injected into the one-cell stage *C. intestinalis* embryo, the *pk*-MO closely copied the *C. savignyi aim* phenotype (Fig. 6A). In *pk*-MO injected *C. intestinalis* embryos we observed stretches of cells that failed to intercalate, as well as stretches that completed intercalation but displayed disrupted nuclear polarity (red arrowheads, Fig. 6A). The *pk*-MO likely knocks down Pk activity from the onset of its expression at gastrula stage (and hence the disruption to intercalation). However, since the nuclear polarization phenotype is not evident until the completion of intercalation, the disruption in A/P polarity seen in non-injected cells is due to a lack of Pk activity in neighboring cells during notochord elongation. To test for cell autonomy of the *pk*-knockdown we took advantage of the fixed and well-characterized cleavage patterns of the *Ciona* embryo (Nishida, 1987). The first cleavage invariably divides the embryo into right and left halves, with each half contributing 20 notochord cells (Fig. 6B). During mediolateral intercalation, notochord cells from the left and right sides interdigitate, alternating in a nearly regular pattern, although it is common to find examples in which two right and then two left notochord cells are found together. In the first experiment, we co-injected the *pk*-MO, along with a fluorescent tracer, into a single blastomere (right or left) at the two-cell stage to create a *pk*-MO mosaic (Fig. 6B). If polarity mechanisms are cell autonomous, we would expect that only those cells containing the morpholino would have polarity defects. Instead, cells from the uninjected side also showed polarity defects (Fig. 6C). This result is consistent with the transmission of cell polarity through local mechanisms between neighboring cells.

To investigate the transmission of polarity along the A/P axis, we made use of the fact that the second cleavage plane results in

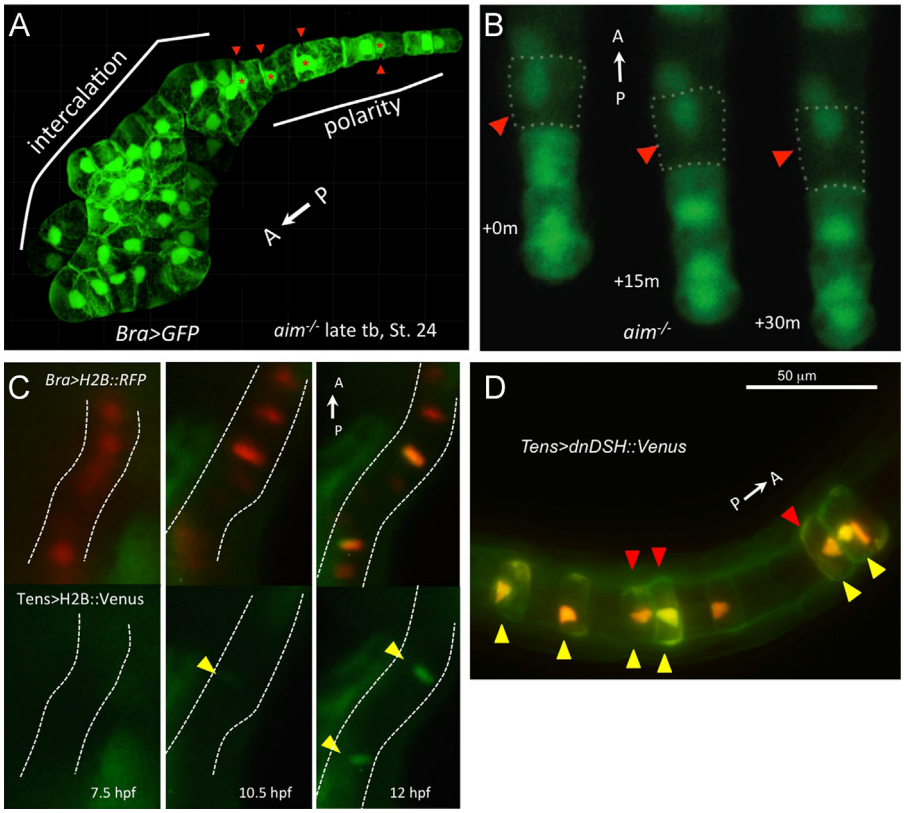

Fig. 5. (A) *The aimless*$^{-/-}$ phenotype typically shows incomplete intercalation in the primary notochord lineage (the anterior 32 cells) and nuclear polarity defects in the secondary lineage (posterior 8 cells). Red arrowheads indicate cells with anterior localization of nuclei (indicated by red asterisks). (B) Although randomization of nuclear placement is seen in *aim*$^{-/-}$ mutants, nuclei are observed to polarize in a manner similar to nuclei of wild type animals – whether anterior or posterior – first extending across the cell, then resolving to the membrane. Figure shows nucleus in an *aim*$^{-/-}$ animal localizing to the anterior. (C) The *Tensin* promoter is later acting than the *Brachyury* promoter. The upper panels show *Bra > H2A::RFP* merged with *Tens > H2A::Venus* and the lower panels shows *Tens > H2A::Venus* alone; both of these constructs label notochord nuclei. Dotted lines represent the approximate lateral boundaries of the notochord. While the *Brachyury* construct can be detected earlier than gastrula stage (not shown here), *Tens > H2A::Venus* is detectable only by about 10.5 hpf, about stage 21, after intercalation is complete. (D) Mosaic expression of dominant-negative *dishevelled* (dnDSH) fused to Venus in the notochord. Polarity defects are seen in expressing cells. Fusion proteins were detected by antibody staining. Yellow: *Tens > dnDSH::Venus*. Red: *BraP > H2A::RFP*. Green: phallacidin. Cells expressing dnDSH from the late-notochord *Tensin* promoter are indicated with yellow arrowheads. Cells with mispolarized nuclei (anterior) are indicated with red arrowheads.

an A/P division of the embryo. The anterior pair of blastomeres gives rise to the anterior thirty-two cells of the notochord, while the posterior two blastomeres give rise to the posterior eight notochord cells (Fig. 6B). When we injected a single anterior blastomere at the four-cell stage and allowed embryos to reach stage 23, both labeled notochord cells and their immediate neighbors in the anterior notochord lineage displayed intercalation defects (Fig. 6D, yellow arrows). However, polarity defects were observed in only 3 of 129 uninjected posterior cells (i.e., the approximate frequency observed in wild-type embryos), and no defects were seen in posterior cells immediately abutting the injected cells ($n=9$ cells), indicating the cell–cell signaling mediated by Pk does not travel from anterior to posterior. Injection of *pk*-MO into a single posterior blastomere of the four-cell embryo resulted in mispolarization of cells ($n=5$ cells) abutting the MO-containing cells ("proximal" view, Fig. 6E), but cells more distant from the injected cells had no visible nuclear polarity defects ("distal" view, Fig. 6E). In summary, we observed non-cell autonomous effects of *pk*-MO knockdown, but these effects appeared to be limited to anterior neighbors, we never observed a cascading wave of mispolarity. In fact, we saw no cases of the non-autonomous knockdown acting at more than two cells lengths ($n=18$ cells). These results are consistent with the core PCP pathway acting at a strictly local level in the *Ciona* notochord to keep the polarity of anterior neighboring cells in register.

Both halves of bisected embryos show normal polarity

The *pk*-MO knockdown experiments indicate that notochord cells signal to their anterior neighbors via the PCP pathway. This mosaic disruption of PCP signaling within the column of cells results in only a local disruption of polarity, rather than a complete loss of polarity anterior to the disruption. Additionally, Pk expression is restricted to the notochord (Hotta et al., 2000), meaning that PCP signaling is not likely to bypass the disruption through surrounding tissues. This would argue against a model in which a posteriorly-localized polarity cue is relayed along the length of the notochord, despite the fact that a number of *Ciona* genes are expressed at the posterior end of the tail, including *wnt5*, *fgf8/17/18*, *tgf-β2* and *Hox12* (Imai et al., 2004; Reeves et al., 2014). If these or other genes were to provide a directional polarizing signal, e.g., by acting as a diffusible morphogen from the posterior (or anterior) of the embryo, it should be possible to isolate one half of the embryo from this signal by embryo bisection (i.e., after bisection through the middle of the tail, only one half of the notochord would maintain contact with the signal, while the other would be isolated from it).

When we bisected the notochord of late-tailbud stage embryos (early stage 23), nuclear polarity was maintained in all of the non-tip notochord cells in both halves when imaged up to 60 min following the bisection (Fig. 7A and B). The notable exception to

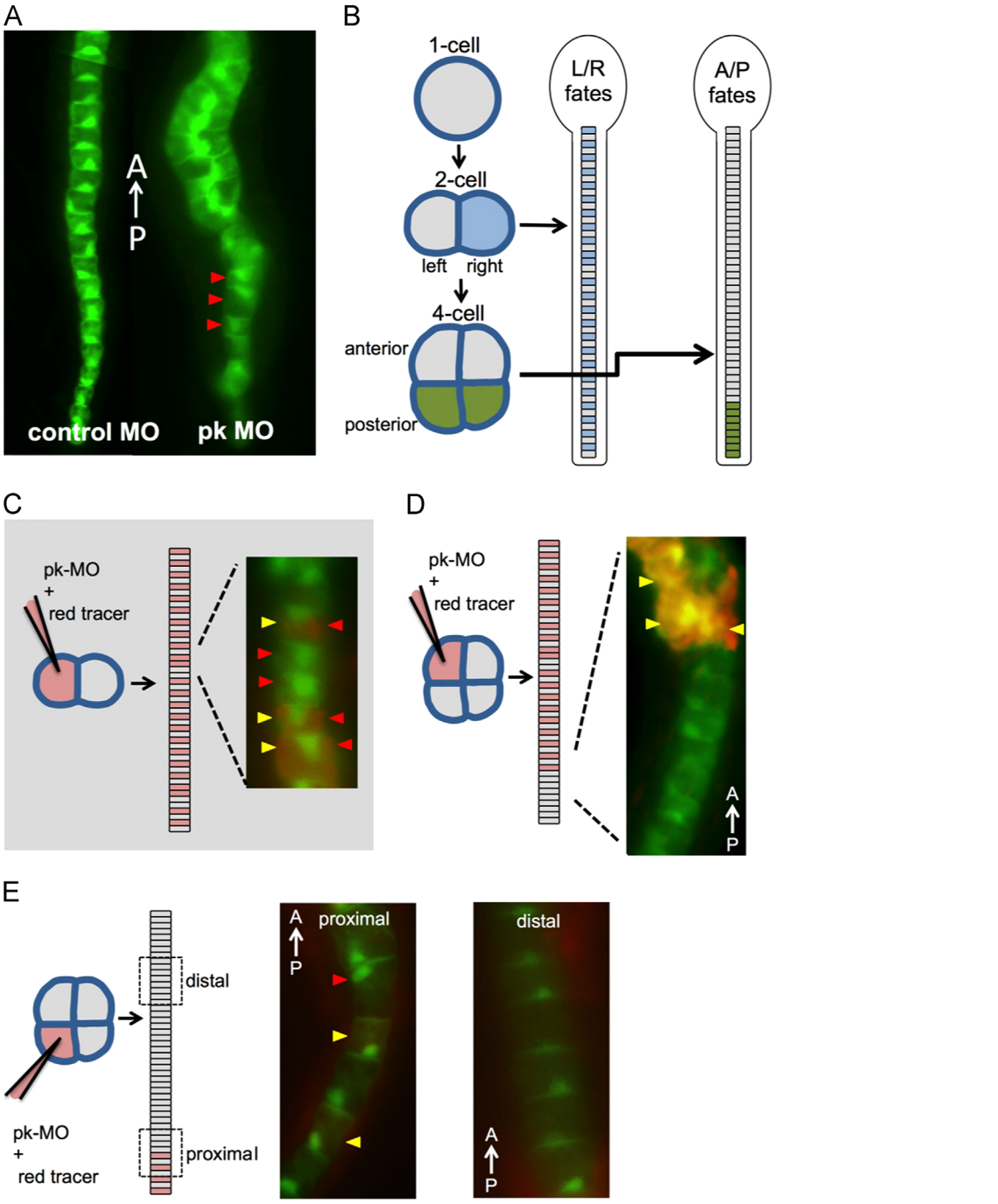

Fig. 6. (A) Injection of an antisense *prickle* morpholino oligonucleotide (pk-MO) in *Ciona intestinalis* phenocopies the *Ciona savignyi aimless* mutation. (B) Two- and four-cell stage cell lineage of the *Ciona* notochord. (C) Injection of pk-MO into one cell of a two cell-stage embryo results in non-cell autonomous disruption of polarity. (D) Injection of the pk-MO into an anterior cell does not disrupt polarity in cells posterior to the injection. (E) Injection of the pk-MO into a posterior cell leads to non-cell autonomous disruption of polarity proximal to the injected cells, but not distally. In all panels red arrowheads indicate cells with mispolarized nuclei and yellow arrowheads indicate cells injected with red tracer used to mark cells receiving the pk-MO. Anterior is at the top for all panels.

this was the newly created posterior-most cells of the anterior halves. The nuclei of these cells relocated to the anterior side, usually within 40 min (Fig. 7A; Suppl. Movie 2). The fact that the remainder of the cells in the anterior half maintained proper polarity argues against the presence of a localized signaling center at the posterior pole. We also examined the expression of *wnt5* approximately 60 min following bisection. We observed no *wnt5* expression in the new posterior pole of the anterior half of the embryo (data not shown), arguing that genes normally expressed in the posterior pole do not become activated in the new posterior pole of the anterior half.

Supplementary material related to this article can be found online at http://dx.doi.org/10.1016/j.ydbio.2014.08.023.

While the above experiment was performed on embryos in which the A/P polarity had already been established, we observed a similar result when embryos where bisected at the neurula stage, well before notochord cell intercalation and A/P polarity is evident in either nuclei position or *Pk::myc* localization. The

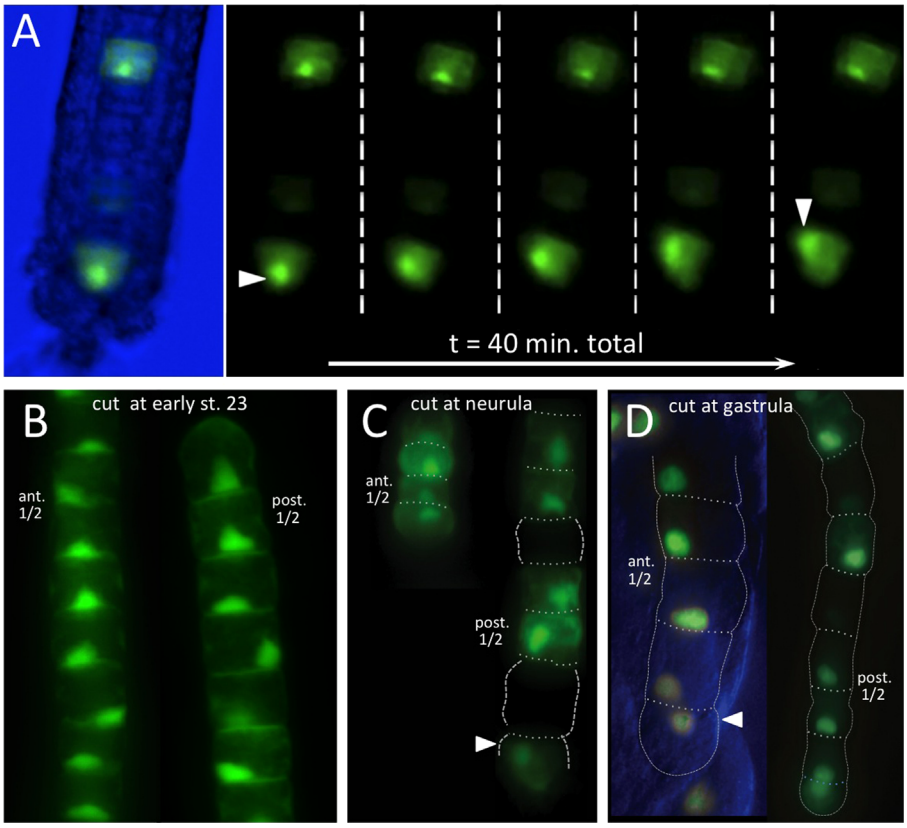

Fig. 7. (A) Relocalization of a nucleus (white arrowhead) in the rostral (anterior) half following bisection at stage 23. (B) With the exception of the new posterior tip cell (A), the other cells of embryos bisected at stage 23 show no change in polarity. Anterior (ant.) and posterior (post.) halves are shown one-hour following bisection. (C) Neurula stage bisections do not disrupt coordinated polarity, as assessed by nuclear position, in either the anterior (rostral) or posterior (caudal) isolates. Note, however, that the final cell of the anterior isolate is placed at the anterior membrane (red arrowhead), like the native posterior tip cell—the only cell to have anterior nuclear placement in a normal, uncut context. (D) Even when the embryo bisection is performed earlier, at the gastrula stage, global nuclear position is not disrupted in anterior or posterior halves. However, as for the neurula bisection, the nucleus of the tip cell of the rostral portion is placed at the anterior pole, not the posterior (red arrowhead). Anterior is up in all panels.

embryo halves, anterior and posterior, continued development and in each half notochord cells were able to complete intercalation. Nuclear polarity appeared unaffected in both anterior and posterior isolates as assessed at the equivalent of stage 23 (Fig. 7C). We performed bisections even earlier, at the gastrula-stage, cutting embryos across the future A–P axis. Even at this stage – when the ten notochord precursors had yet to undergo two final rounds of cell division and had not coalesced to a plate – the bisections yielded embryo halves at stage 23 containing partial notochords with properly polarized cells (Fig. 7D). It remains at least formally possible that a still earlier signal exists; maternal PEM protein, for example, is required for unequal blastomere cleavages and is localized to the posterior pole shortly after fertilization (Prodon et al., 2007; Yoshida et al., 1996). However, the complex sequence of notochord development, including multiple cell divisions, fate determination, considerable morphogenesis, and the lack of any apparent A–P polarity until after intercalation, makes a causal link to any such early signal tenuous. We favor the hypothesis that our results indicate a distributed polarizing signal.

Cell ablation: Dynamic repolarization of cells

The relocalization of nuclei in the newly created posterior tip cells of bisected embryos appears to demonstrate a continuous and dynamic requirement for A/P cell-to-cell signaling in the maintenance of polarity. To further investigate cell-to-cell signaling, single cells in the notochord were killed by laser ablation. Fig. 8 and Suppl. Movie 3 shows an example in which a single cell near the center of the notochord was ablated. To our surprise we observed that the ablated cells (asterisk, Fig. 8) where often extruded from the notochord column, after which the two cells on each side of the ablation adhered to one another, reconstituting the notochord. During this process, we observed that the nucleus of the cell at the anterior side of the gap initially moved to the anterior side of the cell, as if it had no posterior neighbor. Although faint at this particular confocal plane, the nucleus of the cell at the posterior side of the ablation remains at the posterior end of the cell (e.g., yellow arrow at $t=72$ min.). Focusing attention back to the cell at the anterior side of the ablation, it can be seen that after its nucleus contacts the anterior membrane of the cell, between $t=96$ and $t=126$ min, it returns to the posterior, stretching backwards and assuming the characteristic flattened shape where it meets the membrane, presumably due to the reestablished signaling from the repaired connection to its new posterior neighbor. A second example is shown in Suppl. Movie 4. In contrast, Suppl. Movie 5 shows an example in which the ablated cell is not eliminated, in which case the nucleus of the cell anterior to the ablation moves to the anterior and remains.

Supplementary material related to this article can be found online at http://dx.doi.org/10.1016/j.ydbio.2014.08.023.

The results of the bisection and the ablation are consistent with the directionality of signaling being from the posterior cell to the anterior cell. Additionally, these results indicate that the signaling between neighboring cells is present in the fully elongated notochord, rather than a case in which, for example, a polarity bias is only present at the onset of, or during, the elongation phase.

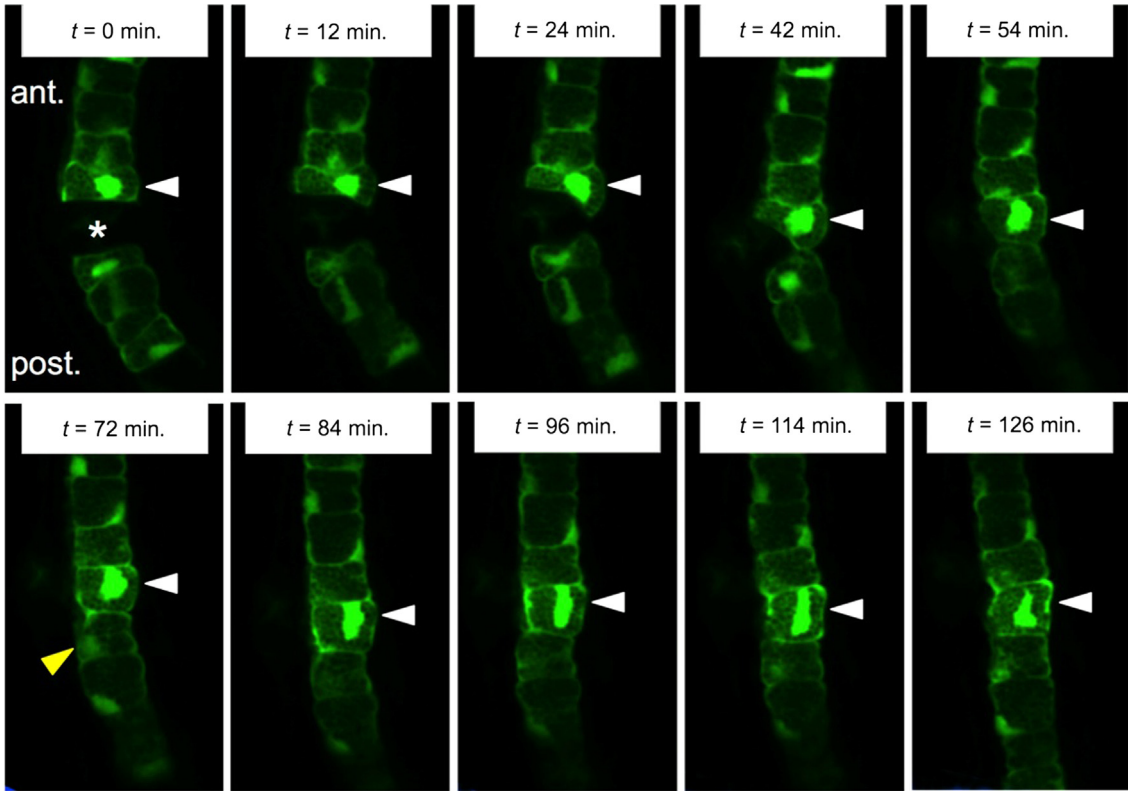

Fig. 8. Lesion and repair in the notochord following laser ablation of a single cell (marked by asterisk). Note the movement of the nucleus of the cell anterior to the lesion (white arrowhead) as it first moves anterior, and then posterior as the junction is restored to its posterior neighbor. Yellow arrowhead at $t=72$ min indicates the nucleus of the cell posterior to the lesion.

Although knockdown of *pk* disrupts the polarity of neighboring cells in a non-cell autonomous manner, disruption at greater distance was not observed.

Discussion

During morphogenesis the *Ciona* notochord undergoes a rapid transition in cell polarization from mediolateral during intercalation to anterior–posterior during elongation. These two phases of notochord polarity, at right angles to each other, appear to be distinct. During mediolateral intercalation no sign of A/P polarity or bias has yet been observed, neither in the subcellular localization of PCP gene products, in actin-based protrusive activity, in cell shapes – which are extended in the M/L axis during intercalation – nor in the sequence of intercalation (Jiang and Smith, 2005; Veeman and Smith, 2013). Moreover, we can manipulate A/P polarity in the post-intercalation notochord by late expression of dominant negative *Dsh*, and by embryo bisection and cell ablation (as seen in newly-created posterior cells), indicating that A/P polarity signals are acting after the completion of intercalation.

Properties of propagation of the polarizing signal in the notochord

A cell-to-cell relay is perhaps the simplest model to describe the entrainment of A/P polarity within the notochord; under this model polarity is transmitted through the single-file grouping of cells, one cell transmitting a polarity state or polarity information to its neighbor, and that cell, in turn, to the next cell, and so on along the length of the notochord. When embryos are mosaically injected with the pk-MO, uninjected cells were observed to show mispolarized nuclei when their posterior neighbors inherited the pk-MO. This result lends support to the importance of local PCP-dependent interactions, as observed in other organisms, particularly the fly where clonal disruption of PCP causes polarity defects in non-mutant neighboring cells [see e.g., (Gubb and Garcia-Bellido, 1982; Taylor et al., 1998)]. However, we never observed polarity defects extending beyond one or two cells from a MO-containing cell, showing that while a posterior neighbor can influence a cell's polarity state, a separate, more general signal may ensure that the polarity of the remaining cells are not disrupted and remain in register. Consistent with this is the observation that mispolarized cells in control animals (occurring at a rate of about 1.3%; see Fig. 1D) are not observed as loci seeding mispolarization throughout the notochord. While these results argue most directly against a long range cell–cell relay, they suggest at the same time a global polarizing signal, an as yet unidentified factor, distributed across the embryonic axis, which influences polarity at a broader scale than the cell–cell interactions seen with the pk-MO experiments.

In *Drosophila*, the organism in which PCP patterning is most widely studied, the nature of the global signal remains unresolved. Proposed global signals in *Drosophila* include the Fat/Dachsous and Wnt pathways (Casal et al., 2006; Thomas and Strutt, 2012; Wu et al., 2013). Another model links the global polarized alignment and distribution of PCP proteins to mechanical events in the *Drosophila* wing (Eaton and Julicher, 2011). Although the morphogenetic movements in the *Ciona* notochord are much simpler than in the *Drosophila* wing, a similar mechanism is possible—the shift in polarity from M/L to A/P in the *Ciona* notochord corresponds to a switch in cell behavior from intercalation to elongation. However, a simple model in which the timing of completion of intercalation translates into A/P polarity is not supported by the observation that the completion of intercalation follows neither an A to P, nor a P to A progression. Rather, the two ends of the notochord complete intercalation first, followed by the middle (Veeman and Smith,

2013). Additionally, we observed the anterior localization of *Pk::myc* at the onset of elongation (stage 22), and before the nuclei are visibly polarized, arguing that the physical events of elongation itself are unlikely to be responsible for localizing PCP components.

Determining directionality for the notochord polarizing signal

Despite the suggestive localization of candidate polarizing molecules, such as wnt5, at the posterior tip of the tail (Imai et al., 2004), our embryo bisection experiments argued against a localized polarizing source acting along the length of the notochord, in either direction. Rather we observed cell-to-cell polarity signaling acting only locally, between neighboring cells. The original observation consistent with this hypothesis is that the posterior-most notochord cell (i.e., the only cell without a posterior neighbor) is also the only cell that behaves differently than the others. In the absence of a posterior neighbor, the posterior tip cell also shows a much higher variability in nuclear placement than other notochord cells; 98.7% of the nuclei in the middle 38 notochord cells were posteriorly polarized, while in the posterior tip cell 76.2% of nuclei were anterior and 23.8% were posterior. Adding another point of comparison, nuclei within anterior tip cells were found to be posteriorly-placed 92.2% of cells examined. We surmise that the presence of a posterior neighbor stabilizes polarity in the cell lying anterior, while a distributed, global signal entrains polarity irrespective of the neighbor relationships of cells. The pk-MO injection data are consistent with this—MO injections restricted to the anterior notochord cells had no effect on posterior cells, whereas injections confined to the posterior could alter polarity in anterior cells, albeit only at a local level. This directionality is reminiscent of the directional, domineering non-autonomy observed for some core PCP components in *Drosophila* (Amonlirdviman et al., 2005), but will have to be further assessed to determine whether broad conservation is shared within the varying geometries of these organisms.

The relocalization of nuclei following bisection and laser photoablation provides additional support for a posterior-to-anterior direction for a local polarizing signal; both manipulations place the notochord cell anterior to the cut in a new context, namely, they make that cell more like the native posterior tip cell by removing the cell's posterior neighbor. If polarity were imparted anterior to posterior, no difference in nuclear polarity would be expected after a cut or ablation, as the signaling cell, that cell immediately anterior, remains intact and uninterrupted. At the same time, the cell on the posterior side of the cut – that cell in the posterior isolate that is deprived of its anterior neighbor – was never observed to change its nucleus position (Fig. 4). This was true whether the bisection was performed at gastrula or post-polarization stages. After the cut, this cell is also found in a new context, without an anterior neighbor, yet its polarity remained unperturbed. In the photoablation shown in Fig. 8, a cell's neighbor relations were observed to change twice: once when the posterior cell was removed causing a shift of the nucleus to the anterior membrane, and a second time when the notochord was reconstituted, at which time the nucleus returned to the posterior pole. These observations are consistent with polarity information travelling from posterior to anterior, but not from anterior to posterior.

Summary

We have presented results showing the *Ciona* notochord to be a highly tractable model for real-time imaging and manipulation of the PCP pathway. The position of the nucleus provides a rapid and dynamic read-out of the polarization of the notochord cell, and A/P polarization of nuclei still occurs in the absence of Pk, although in a randomized rather than coordinated manner. Simplifying the characterization of the PCP pathway in *Ciona* is the fact that morphogenesis of the notochord occurs with only forty post-mitotic cells. The cells first undergo a medially-directed intercalation, and then develop a robust anterior/posterior polarity. The cells of the post-intercalation notochord show polarity in a single and static dimension, and morphogenesis for the period studied is limited to a simple elongation of the cells in the axis of polarization. Complicating the analysis of the PCP pathway in other species are shifting axes, seen for example in the growing *Drosophila* wing, and overlapping genetic components that function both in PCP signaling and in the growth-promoting Hippo pathway. While genes acting in the Hippo pathway appear to be present in the *Ciona* genome (Hilman and Gat, 2011), the *Ciona* notochord neither increases appreciably in volume (Veeman and Smith, 2013), nor undergoes mitoses at these stages, suggesting that much of the confusion regarding polarity versus the simultaneous signaling for cellular growth (Matakatsu and Blair, 2012) may not be present.

Acknowledgments

This work was supported by award GM088997 from the National Institutes of Health. We thank Mary Raven and acknowledge the use of the NRI-MCDB Microscopy Facility and the Multiphoton/Laser Scanning Confocal supported by the NCRR, National Institutes of Health of the NIH, under Award RR022585.

References

Amonlirdviman, K., Khare, N.A., Tree, D.R., Chen, W.S., Axelrod, J.D., Tomlin, C.J., 2005. Mathematical modeling of planar cell polarity to understand domineering nonautonomy. Science 307, 423–426.
Axelrod, J.D., Miller, J.R., Shulman, J.M., Moon, R.T., Perrimon, N., 1998. Differential recruitment of Dishevelled provides signaling specificity in the planar cell polarity and Wingless signaling pathways. Genes Dev. 12, 2610–2622.
Axelrod, J.D., Tomlin, C.J., 2011. Modeling the control of planar cell polarity. Wiley interdisciplinary reviews. Syst. Biol. Med. 3, 588–605.
Bertet, C., Lecuit, T., 2009. Planar polarity and short-range polarization in Drosophila embryos. Semin. Cell Dev. Biol. 20, 1006–1013.
Casal, J., Lawrence, P.A., Struhl, G., 2006. Two separate molecular systems, Dachsous/Fat and Starry night/Frizzled, act independently to confer planar cell polarity. Development 133, 4561–4572.
Chang, H., Nathans, J., 2013. Responses of hair follicle-associated structures to loss of planar cell polarity signaling. Proc. Natl. Acad. Sci. U.S.A. 110, E908–917.
Christiaen, L., Wagner, E., Shi, W., Levine, M., 2009. Electroporation of transgenic DNAs in the sea squirt Ciona. Cold Spring Harbor Protoc. 2009 (pdb prot5345).
Corbo, J.C., Levine, M., Zeller, R.W., 1997. Characterization of a notochord-specific enhancer from the Brachyury promoter region of the ascidian, *Ciona intestinalis*. Development 124, 589–602.
Deschet, K., Nakatani, Y., Smith, W.C., 2003. Generation of Ci-Brachyury-GFP stable transgenic lines in the ascidian *Ciona savignyi*. Genesis 35, 248–259.
Eaton, S., Julicher, F., 2011. Cell flow and tissue polarity patterns. Curr. Opin. Genet. Dev. 21, 747–752.
Ezan, J., Montcouquiol, M., 2013. Revisiting planar cell polarity in the inner ear. Semin. Cell Dev. Biol. 24, 499–506.
Goodrich, L.V., Strutt, D., 2011. Principles of planar polarity in animal development. Development 138, 1877–1892.
Gubb, D., Garcia-Bellido, A., 1982. A genetic analysis of the determination of cuticular polarity during development in *Drosophila melanogaster*. J. Embryol. Exp. Morphol. 68, 37–57.
Hendrickson, C., Christiaen, L., Deschet, K., Jiang, D., Joly, J.S., Legendre, L., Nakatani, Y., Tresser, J., Smith, W.C., 2004. Culture of adult ascidians and ascidian genetics. Methods Cell Biol. 74, 143–170.
Hilman, D., Gat, U., 2011. The evolutionary history of YAP and the hippo/YAP pathway. Mol. Biol. Evol. 28, 2403–2417.
Hotta, K., Mitsuhara, K., Takahashi, H., Inaba, K., Oka, K., Gojobori, T., Ikeo, K., 2007. A web-based interactive developmental table for the ascidian *Ciona intestinalis*, including 3D real-image embryo reconstructions: I. From fertilized egg to hatching larva (An Official Publication of the American Association of Anatomists). Dev. Dyn. 236, 1790–1805.
Hotta, K., Takahashi, H., Asakura, T., Saitoh, B., Takatori, N., Satou, Y., Satoh, N., 2000. Characterization of Brachyury-downstream notochord genes in the *Ciona intestinalis* embryo. Dev. Biol. 224, 69–80.

Hotta, K., Takahashi, H., Erives, A., Levine, M., Satoh, N., 1999. Temporal expression patterns of 39 Brachyury-downstream genes associated with notochord formation in the *Ciona intestinalis* embryo. Dev. Growth Differ. 41, 657–664.

Imai, K.S., Hino, K., Yagi, K., Satoh, N., Satou, Y., 2004. Gene expression profiles of transcription factors and signaling molecules in the ascidian embryo: towards a comprehensive understanding of gene networks. Development 131, 4047–4058.

Jiang, D., Munro, E.M., Smith, W.C., 2005. Ascidian prickle regulates both mediolateral and anterior–posterior cell polarity of notochord cells. Curr. Biol.: CB 15, 79–85.

Jiang, D., Smith, W.C., 2005. Self- and cross-fertilization in the solitary ascidian *Ciona savignyi*. Biol. Bull. 209, 107–112.

Jiang, D., Smith, W.C., 2007. Ascidian notochord morphogenesis (An Official Publication of the American Association of Anatomists). Dev. Dyn. 236, 1748–1757.

Joly, J.S., Kano, S., Matsuoka, T., Auger, H., Hirayama, K., Satoh, N., Awazu, S., Legendre, L., Sasakura, Y., 2007. Culture of *Ciona intestinalis* in closed systems (An Official Publication of the American Association of Anatomists). Dev. Dyn. 236, 1832–1840.

Keller, R., Davidson, L., Edlund, A., Elul, T., Ezin, M., Shook, D., Skoglund, P., 2000. Mechanisms of convergence and extension by cell intercalation. Philos. Trans. R. Soc. London, Ser. B 355, 897–922.

Matakatsu, H., Blair, S.S., 2012. Separating planar cell polarity and Hippo pathway activities of the protocadherins Fat and Dachsous. Development 139, 1498–1508.

Munro, E.M., Odell, G., 2002. Morphogenetic pattern formation during ascidian notochord formation is regulative and highly robust. Development 129, 1–12.

Nakatani, Y., Nishida, H., 1999. Duration of competence and inducing capacity of blastomeres in notochord induction during ascidian embryogenesis. Dev. Growth Differ. 41, 449–453.

Nishida, H., 1987. Cell lineage analysis in ascidian embryos by intracellular injection of a tracer enzyme. III. Up to the tissue restricted stage. Dev. Biol. 121, 526–541.

Prodon, F., Yamada, L., Shirae-Kurabayashi, M., Nakamura, Y., Sasakura, Y., 2007. Postplasmic/PEM RNAs: a class of localized maternal mRNAs with multiple roles in cell polarity and development in ascidian embryos (An Official Publication of the American Association of Anatomists). Dev. Dyn. 236, 1698–1715.

Reeves, W., Thayer, R., Veeman, M., 2014. Anterior–posterior regionalized gene expression in the Ciona notochord (An Official Publication of the American Association of Anatomists). Dev. Dyn. 243, 612–620.

Roure, A., Rothbacher, U., Robin, F., Kalmar, E., Ferone, G., Lamy, C., Missero, C., Mueller, F., Lemaire, P., 2007. A multicassette Gateway vector set for high throughput and comparative analyses in ciona and vertebrate embryos. PLoS One 2, e916.

Schindelin, J., Arganda-Carreras, I., Frise, E., Kaynig, V., Longair, M., Pietzsch, T., Preibisch, S., Rueden, C., Saalfeld, S., Schmid, B., Tinevez, J.Y., White, D.J., Hartenstein, V., Eliceiri, K., Tomancak, P., Cardona, A., 2012. Fiji: an open-source platform for biological-image analysis. Nat. Methods 9, 676–682.

Seifert, J.R., Mlodzik, M., 2007. Frizzled/PCP signalling: a conserved mechanism regulating cell polarity and directed motility. Nat. Rev. Genet. 8, 126–138.

Shi, W., Peyrot, S.M., Munro, E., Levine, M., 2009. FGF3 in the floor plate directs notochord convergent extension in the Ciona tadpole. Development 136, 23–28.

Stemple, D.L., 2005. Structure and function of the notochord: an essential organ for chordate development. Development 132, 2503–2512.

Taylor, J., Abramova, N., Charlton, J., Adler, P.N., 1998. Van Gogh: a new Drosophila tissue polarity gene. Genetics 150, 199–210.

Thomas, C., Strutt, D., 2012. The roles of the cadherins Fat and Dachsous in planar polarity specification in Drosophila (An Official Publication of the American Association of Anatomists). Dev. Dyn. 241, 27–39.

Veeman, M.T., Chiba, S., Smith, W.C., 2011. Ciona genetics. Methods Mol. Biol. 770, 401–422.

Veeman, M.T., Smith, W.C., 2013. Whole-organ cell shape analysis reveals the developmental basis of ascidian notochord taper. Dev. Biol. 373, 281–289.

Wallingford, J.B., Fraser, S.E., Harland, R.M., 2002. Convergent extension: the molecular control of polarized cell movement during embryonic development. Dev. Cell 2, 695–706.

Wang, Y., Nathans, J., 2007. Tissue/planar cell polarity in vertebrates: new insights and new questions. Development 134, 647–658.

Wu, J., Roman, A.C., Carvajal-Gonzalez, J.M., Mlodzik, M., 2013. Wg and Wnt4 provide long-range directional input to planar cell polarity orientation in Drosophila. Nat. Cell Biol. 15, 1045–1055.

Yamada, L., Shoguchi, E., Wada, S., Kobayashi, K., Mochizuki, Y., Satou, Y., Satoh, N., 2003. Morpholino-based gene knockdown screen of novel genes with developmental function in *Ciona intestinalis*. Development 130, 6485–6495.

Yoshida, S., Marikawa, Y., Satoh, N., 1996. Posterior end mark, a novel maternal gene encoding a localized factor in the ascidian embryo. Development 122, 2005–2012.